

Supporting Information for

Development of a Transferable Coarse-Grained Model of Polydimethylsiloxane

Sonia Cambiaso, Fabio Rasera Figueredo, Giulia Rossi, and Davide Bochicchio.*

Physics Department, University of Genoa, Via Dodecaneso 33, 16146 Genoa, Italy

*bochicchio@fisica.unige.it

Atomistic model

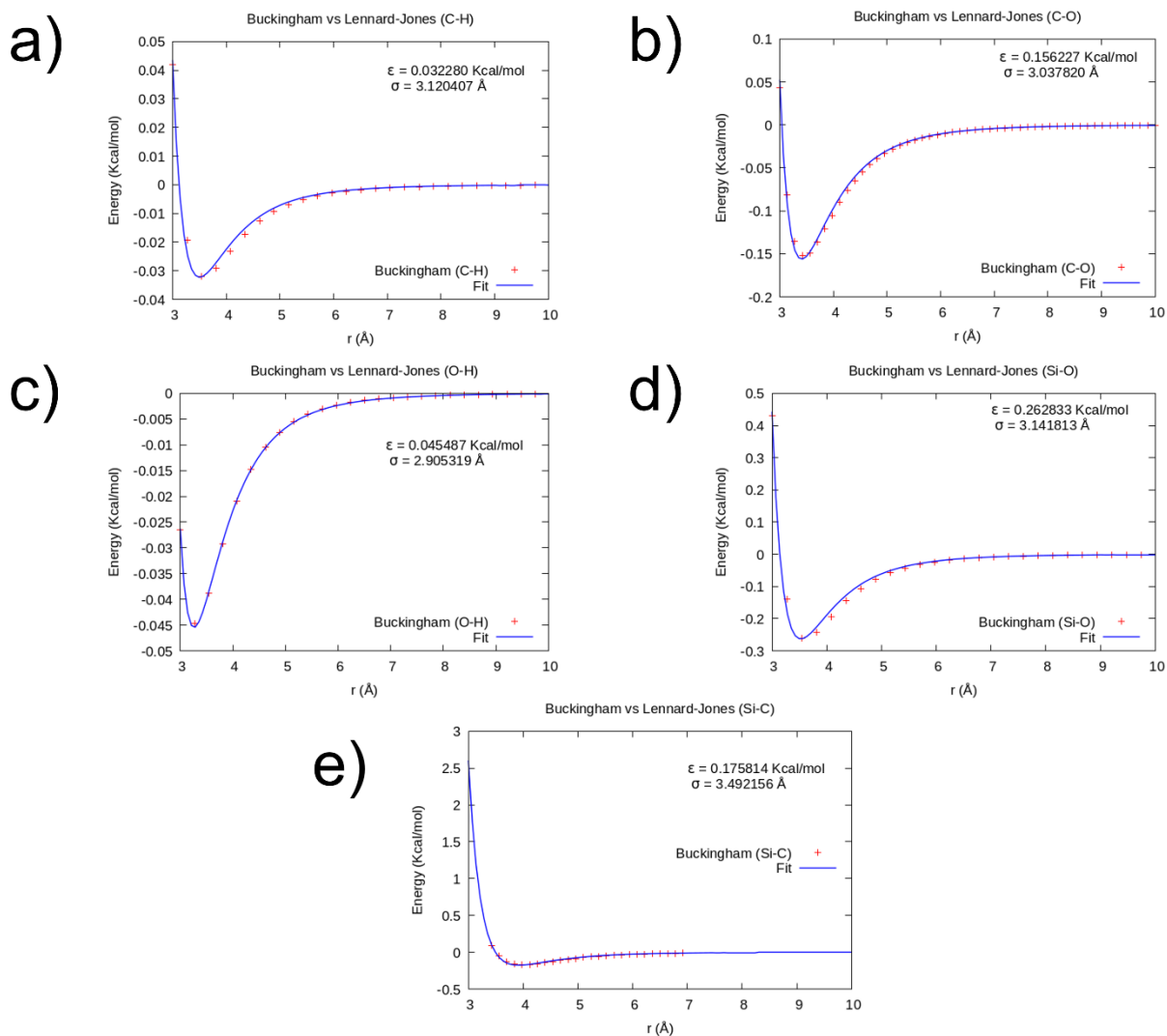


Figure S11. Fit of the Buckingham potential¹ (red points) with a Lennard-Jones potential (blue line) for the mixed interactions. From these fits we obtained the parameters (ϵ , σ) of the LJ potential for the a) C-H, b) C-O, c) O-H, d) Si-O, and e) Si-C interactions. The parameters of the Si-H interaction were calculated with the Lorentz-Berthelot combination rule².

	σ (nm)	ϵ (kJ/mol)
Si-Si	0.3759	0.9962
C-C	0.3345	0.3379
O-O	0.2815	0.8355
H-H	0.2650	0.0383
Si-O	0.3142	1.0997

Si-C	0.3492	0.7356
C-O	0.3038	0.6536
O-H	0.2907	0.1898
C-H	0.3120	0.1351
Si-H	0.3156	0.1953

Table SI1. LJ potential parameters (σ and ϵ) for PDMS atomistic model.

	Atom	q (e)
Core monomers	Si	0.7608
	C	-0.5604
	O	-0.4620
	H	0.1370
Start monomers	Si	0.6792
	C	-0.5603
	H	0.1113
End monomers	Si	0.7608
	C	-0.5604
	O	-0.4620
	H	0.1536

Table SI2. Partial atomic charges for PDMS atomistic model. The partial charges of hydrogens in the end monomer are slightly changed to assure the whole chain neutrality.

		k_b (kJ/mol·nm ²)	b_0 (nm)		
Bonds	Si-O	292880	0.1651		
	Si-C	158992	0.1878		
	C-H	274470	0.1092		
		k_ϑ (kJ/mol)	ϑ_0 (deg)		

Angles	Si-O-Si	118.4	144.0		
	O-Si-O	791.2	109.5		
	O-Si-C	418.4	109.5		
	C-Si-C	418.4	109.5		
	Si-C-H	240.75	111.09		
	H-C-H	322.17	107.77		
		k_φ (kJ/mol)	k_φ (kJ/mol)	k_φ (kJ/mol)	φ_0 (deg)
		($n=1$)	($n=2$)	($n=3$)	
Dihedrals	Si-O-Si-O	0.857720	-0.571510	-0.459570	0
	Si-O-Si-C			0.119369	0
	O-Si-C-H			0.313800	0
	C-Si-C-H			0.313800	0

Table S13. Atomistic PDMS bonded parameters. The parameters b_0 (nm) and k_b (kJ/mol·nm²) are the equilibrium bond length and the elastic constant of the harmonic bond potential. The parameters ϑ_0 (deg) and k_ϑ (kJ/mol) are the equilibrium angle and the elastic constant of the harmonic angle potential. The function used to describe proper dihedral is the following: $V_d(\varphi_{ijkl}) = \frac{1}{2}k_\varphi(1 + \cos(n\varphi - \varphi_0))$, where φ_0 is the equilibrium angle between the ijk and jkl planes, with zero corresponding to the *cis* configuration, and n the multiplicity that allows to apply multiple potential functions automatically to a single dihedral.

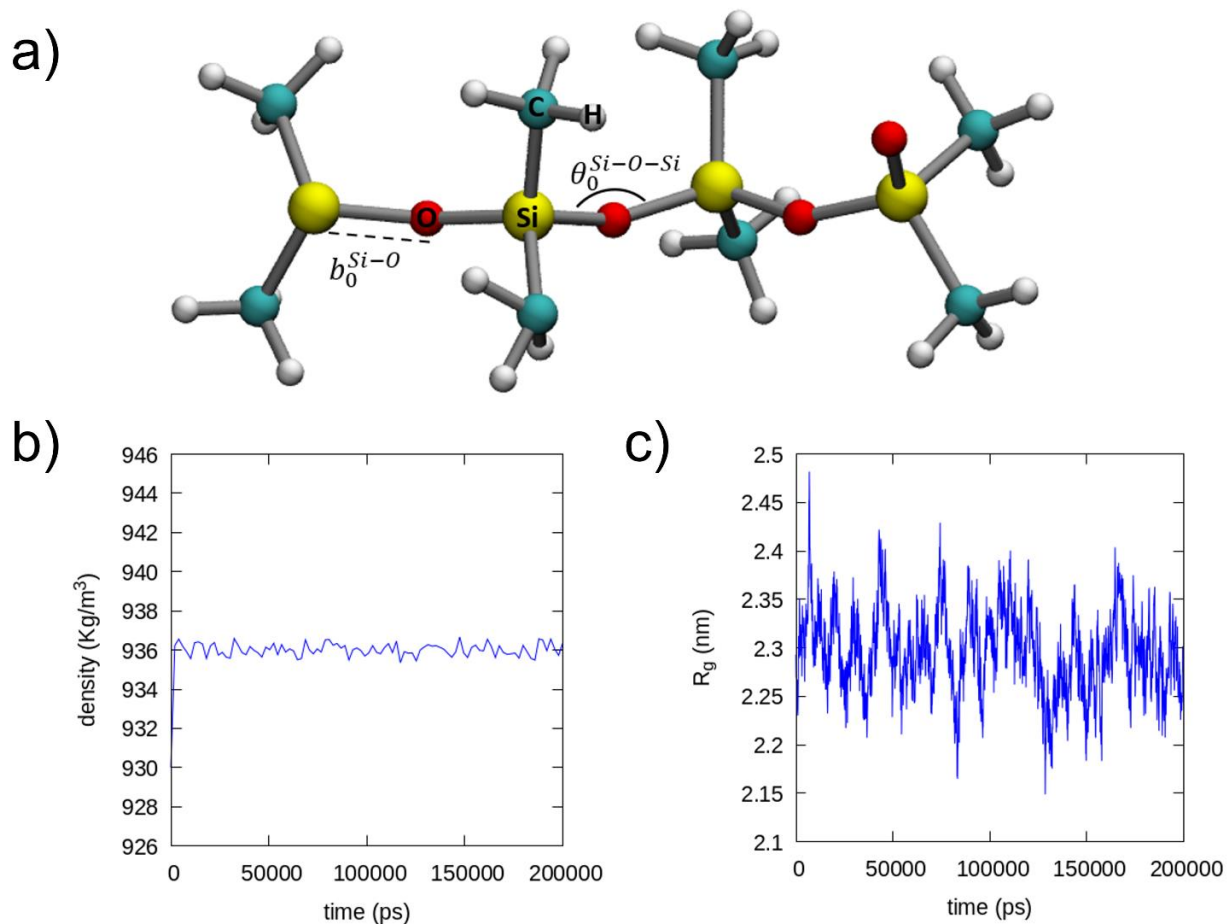


Figure S12. a) Atomistic PDMS structure: silicon is represented in yellow, oxygen in red, carbon in cyan, and hydrogen in grey. The equilibrium length between silicon and oxygen (b_0^{Si-O}) and the equilibrium angle between silicon, oxygen, and silicon ($\theta_0^{Si-O-Si}$) are reported as examples of the bonded parameters of Table S13. Panel b) and c) represent respectively PDMS melt density and gyration radius (R_g) obtained with the atomistic model.

a)	N_{chain}	ρ (kg/m ³)	Experimental ³ ρ (kg/m ³)	Atomistic reference ⁴ ρ (kg/m ³)
	100	936 ± 3		
	200	936 ± 2	935	948 ± 2
	300	936 ± 2		
b)	N	R_g (nm)	Experimental ³ R_g (nm)	Theoretical R_g (nm)
	100	0.89 ± 0.01		
	200	0.892 ± 0.008	$0.687 \div 1.371$	0.944

300	0.891 ± 0.009		
-----	-------------------	--	--

Table SI4. Atomistic model test on structural properties of the melt. a) Density (ρ) of three PDMS17 melts with different numbers of chains (N_{chain}), obtained from our simulations (second column), the experimental measurements, and the reference atomistic model. b) The radius of gyration (R_g) obtained from our simulations (second column), the experimental relation³ ($R_g(\text{\AA}) = (0.22 \pm 0.03)M_W^{(0.53 \pm 0.03)}$), and the theoretical one ($R_g^2 = \frac{Na^2}{6}$), which applies to ideal linear chains. The data referred to the experimental measurements show a wide range of values due to the uncertainties on both the exponential and the proportionality factors. The R_g values found in our simulations with different melt sizes are all included in this interval.

Simulation parameters

	N_d	l_{box} (nm)	t (ns)	N_{pdms}		
AA sim	17	6.1	200	100		
	17	7.7	200	200		
	17	8.8	200	300		
CG sim	17	8.3	200	300		
					N_{water}	
TI	25	-	80	80	1280	
					N_{solv}	Solvent
R_g (CG sim)	10	13	5000	1	18928	Water
	50	13	5000		18928	
	100	19	5000		62192	
	150	19	5000		54080	
	250	19	5000		54080	
	10	12	5000		10400	Cyclohexane
	50	12	5000		10400	
	100	20	5000		46800	
	150	20	5000		46400	

	250	20	5000		43600	
	10	12	5000		10000	Hexane
	50	12	5000		10400	
	100	20	5000		46800	
	150	20	5000		46400	
	250	20	5000		43600	
	10	15	5000		2613	Melt
	50	13	5000		247	
	100	24	5000		981	
	150	24	10000		568	
	250	24	30000		180	

Table S15. PDMS simulation details. Parameters of all the atomistic (AA) and coarse-grained (CG) simulations performed during the development and validation of the PDMS model. N_d is the PDMS degree of polymerization, l_{box} is the average length of the simulation box edge, and t is the simulation time. N_{pdms} , N_{solv} , and N_{water} are the number of PDMS, solvent, and water molecules respectively.

CG model development

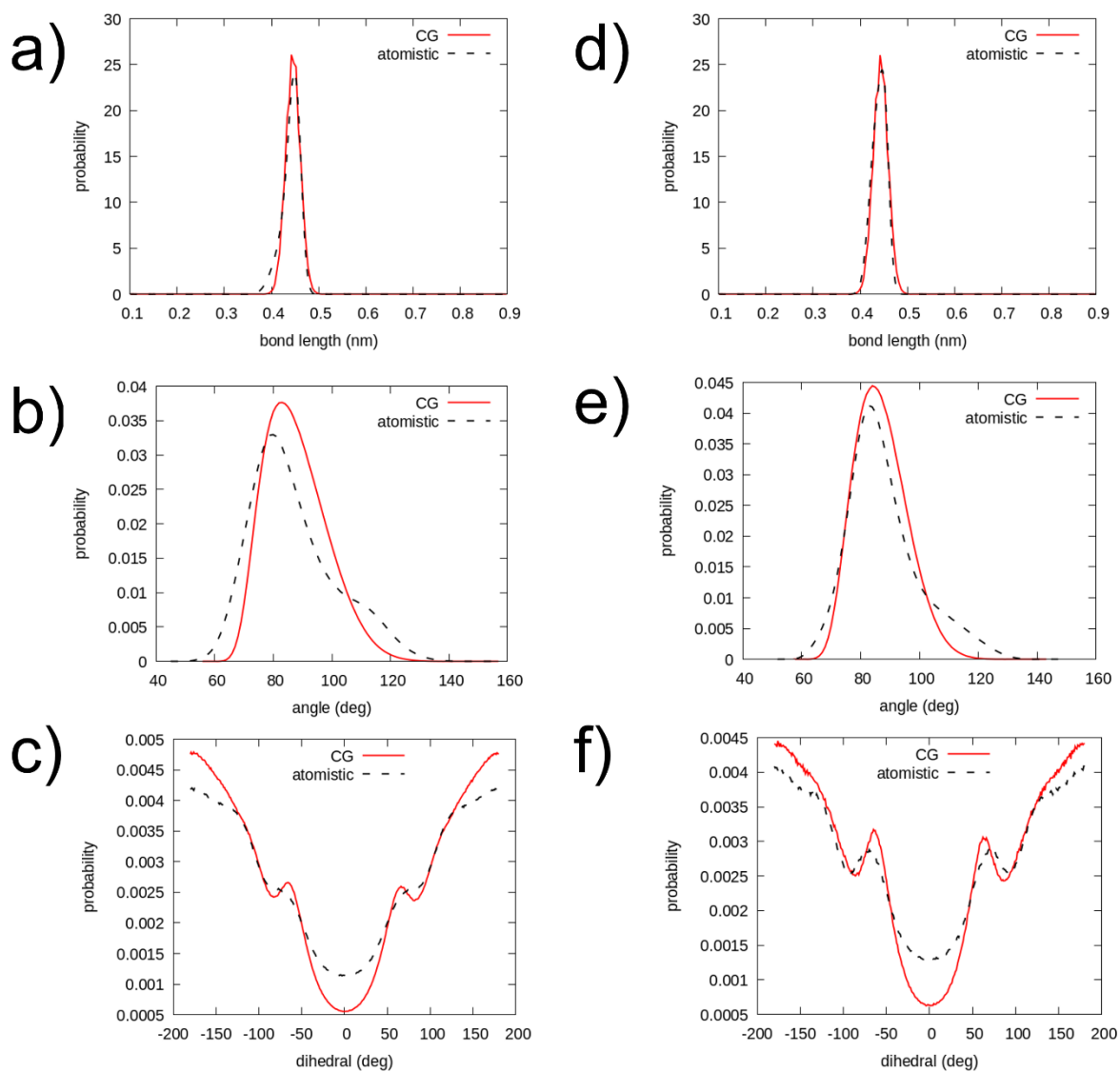


Figure S13. Superposition of atomistic (dashed black line) and CG (red line) distributions of a) bonds, b) angles, and c) dihedrals, relative to core PDMS beads and of d) bonds, e) angles, and f) dihedrals, relative to end PDMS beads.

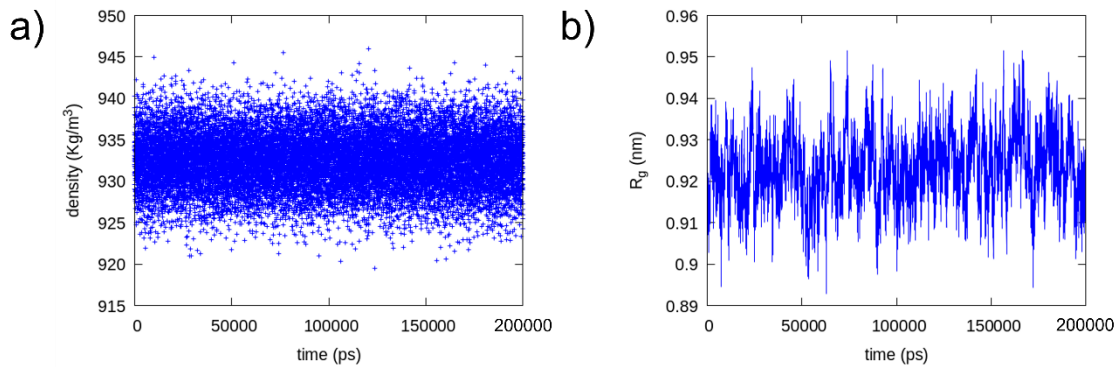


Figure SI4. a) Density and b) gyration radius R_g of the CG PDMS melt composed of 300 chains obtained using the new DMS bead with $\sigma = 0.51$ nm and $\varepsilon = 3.07$ kJ/mol. The results ($\rho = 932 \pm 3$ and $R_g = 0.923 \pm 0.008$) are in good agreement with the atomistic and experimental references.

CG model validation

Solvent	N	R_g (nm)	Standard error (nm)
Water	10	0.561	0.003
	50	0.928	0.001
	100	1.1601	0.0008
	150	1.3224	0.0007
	250	1.5614	0.0006
Cyclohexane	10	0.667	0.003
	50	1.79	0.02
	100	2.56	0.03
	150	3.19	0.04
	250	3.9	0.1
Hexane	10	0.684	0.003
	50	1.89	0.02
	100	2.84	0.03
	150	3.49	0.05
	250	4.58	0.16

PDMS	10	0.66148	0.00007
	50	1.741	0.002
	100	2.515	0.005
	150	3.104	0.005
	250	4.04	0.01

Table SI6. Gyration radius in different solvents with different degree of polymerization.

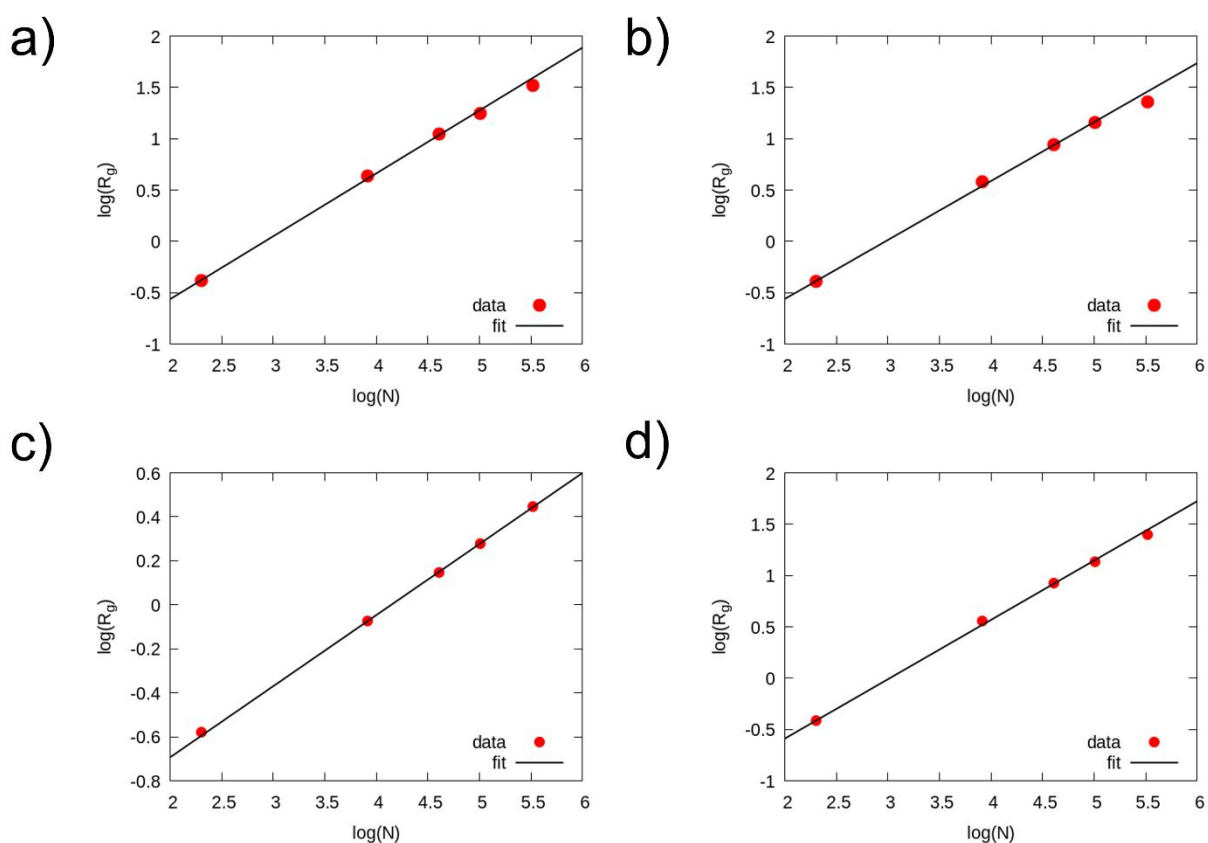


Figure SI5. Scaling law of the gyration radius (R_g) with the degree of polymerization (N) in logarithmic scale for different solvents: a) hexane, b) cyclohexane, c) water, and d) PDMS.

Solvent	ν	Target
Water	0.323 ± 0.001	0.3
Cyclohexane	0.57 ± 0.01	0.6

Hexane	0.613 ± 0.008	0.6
PDMS melt	0.58 ± 0.01	0.53 ± 0.037

Table SI7. Gyration radius in different solvents with different degree of polymerization. For each solvent, the value of ν resulting from the fits in Figure SI5 is reported. The targets result from the theoretical scaling law ($R_g \propto N^\nu$) in the case of hexane, cyclohexane, and water, and the experimental data for PDMS.

Test application

Contact angle

We performed 1 μ s CG simulations in the NVT ensemble at 298 K to compute the contact angle of water/acetonitrile on PDMS. The two simulated systems consisted of a (50x8x5)nm³ PDMS box, made of 305 PDMS₅₀ chain and a cylindrical solvent droplet containing 20848 molecules of water and acetonitrile, respectively. Both solvents are part of the Martini 3 release. In particular, acetonitrile is composed of SN5ah bead. For the water droplet, we used a mix of the three water size beads (regular W, small SW, tiny TW) in equal proportion. The PDMS was first equilibrated, then frozen during the production run, following the procedure used by Boudaghi (ref), to simulate a crosslinked PDMS surface, as the ones used in experiments.

For each solvent we performed five independent runs. In every run, the contact angle was calculated from the last 500 ns of the trajectory. To compute the contact angle, we did a circular cap fit to the isodensity contour that best suited the border of the droplet at the interface with vacuum, using an in-house Python script.

Triblock copolymer

Ibarboure et al.⁵ showed that a variation in the peptide chain length leads to two consequences. On the one hand, shorter chains are more likely to form β -strand structures, while chains with more than 20 units prefer to organize in α -helices. On the other hand, a different ratio between PDMS and PBLG may bring different copolymer morphologies. Following Casey Johnson et al.⁶, we simulated two GSG triblock copolymers with different PBLG compositions (Table SI8) and the same PDMS length. We reported the details of all the systems simulated in this section in Table SI9.

Name	Composition	PBLG secondary structure
GSG5	PBLG ₅ -PDMS ₃₀ -PBLG ₅	Mainly β -strands
GSG20	PBLG ₂₀ -PDMS ₃₀ -PBLG ₂₀	Mainly α -helix

Table SI8. PDMS-PBLG-PDMS triblock (GSG) composition. Composition of the two GSG triblock copolymers used during the simulations. The peptide secondary structure changes according to the chain length.

	l_{box} (nm)	t (ns)	N_d (PBLG)	N_{PBLG}	N_d (PDMS)	N_{GSG}	Annealing
Homoblocks	7.5	200	5	300	-	-	-
	11.8	200	20	300	-	-	-
Triblocks	8.1	900	5		30	67	300 K (400 ns) – 500 K (400 ns) – 300 K (100 ns)
	13.4	4000	20		30	158	300 K (1 μ s) – 500 K (2 μ s) – 300 K (600 ns)

Table SI9. GSG simulations details. Parameters of all the simulations regarding the development of Martini 3 models for the PBGL peptide and the GSG triblocks. l_{box} is the average length of the simulation box edge, t is the simulation time, and N_d is the degree of polymerization. N_{PBLG} and N_{GSG} are respectively the number of PBLG and GSG chains contained in the box. The last column shows the annealing procedure used in the production runs.

PBLG model development

Before simulating the copolymer, we had to build a CG model of PBLG. To do so, we based our choices on the Martini 2 parameters of Casey Johnson⁶ and Knecht⁷, turning them into a Martini 3 model. Figure SI6b shows the mapping we chose for PBLG: a single bead (denoted as BAS) represented the backbone, the acetic acid moiety of the side chain was mapped into an N4a bead (called SID), and we used three TC5 beads (called SI) to represent the benzyl ring. To obtain the two different peptide secondary structures, we varied the bead types for the backbone and the angle and dihedral parameters. In particular, for the short peptide chains that we expected to form β -strands, we used a P2 bead to represent BAS. For the long chains, which we expected instead to constitute α -helices, we mapped the backbone into an N3a bead. The connection between the peptide and PDMS blocks consisted of an N6 bead. Regarding the non-bonded parameters of PBLG, we used the typical Martini 3 energy levels. Table SI10 reports all the bonded parameters relative to PBGL, and Table SI11 shows the PBLG-PDMS bonded and non-bonded interactions.

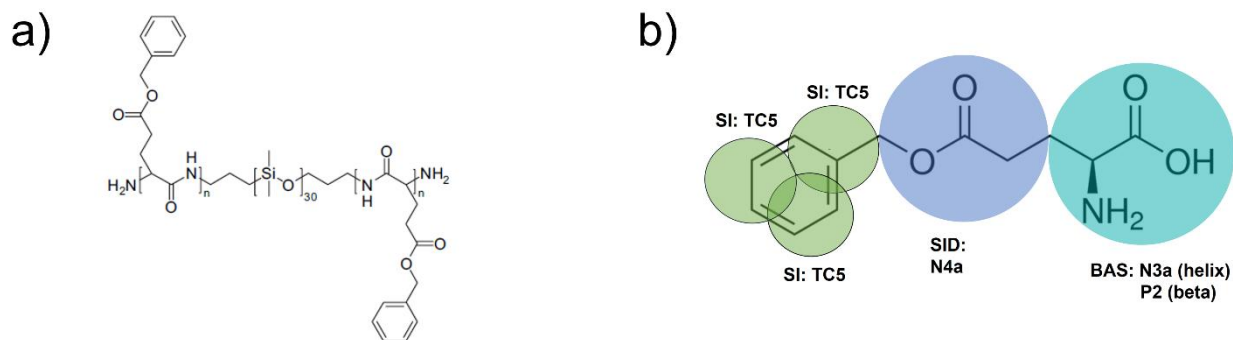


Figure S16. a) Poly(γ -benzyl-L-glutamate)-b-polydimethylsiloxane-b-poly(γ -benzyl-L-glutamate) (GSG) triblock copolymer structure. b) Superposition of poly(γ -benzyl-L-glutamate) (PBLG) atomistic structure and CG mapping: the cyan area represents the backbone bead (BAS), the blue area the side chain ($-CH_2 - COO -$) bead (SID), and the green areas the three TC5 beads of the benzyl ring.

Bonds	k_b (kJ/mol·nm ²)	b_o (nm)	
BAS-BAS	1250	0.35	
BAS-SID	5000	0.4	
SID-SI	7500	0.31	
SI-SI	constraints	0.29	
Angles	k_θ (kJ/mol)	θ_o (deg)	
BAS-BAS-BAS (β -strands)	25	134	
BAS-BAS-BAS (α -helices)	50	96	
SID-BAS-BAS	25	100	
BAS-SID-SI	25	180	
SID-SI-SI	50	150	
Proper Dihedrals	k_ϕ (kJ/mol)	ϕ_o (deg)	n
BAS-BAS-BAS-BAS (β -strands)	10	180	1
BAS-BAS-BAS-BAS (α -helices)	400	60	1
Improper Dihedrals	k_ξ (kJ/mol·rad ²)	ξ_o (deg)	
SID-SI-SI-SI (improper type)	50	0.0	

Table SI10. Martini 3 PBLG parameters. The parameters b_0 (nm) and k_b (kJ/mol·nm²) are the equilibrium bond length and the elastic constant of the harmonic bond potential. The parameters ϑ_0 (deg) and k_ϑ (kJ/mol) are the equilibrium angle and the elastic constant of the harmonic angle potential. The function used to describe proper dihedral is the following: $V_d(\varphi_{ijkl}) = \frac{1}{2}k_\varphi(1 + \cos(n\varphi - \varphi_0))$, where φ_0 is the equilibrium angle between the ijk and jkl planes, with zero corresponding to the *cis* configuration, and n the multiplicity that allows to apply multiple potential functions automatically to a single dihedral. k_ξ and ξ_0 are respectively the elastic constant and the equilibrium angle of the harmonic potential used to describe improper dihedrals. The angle and dihedral parameters relative to the backbone beads have different values to describe the two different secondary structures.

Bonds	k_b (kJ/mol·nm²)	b_0 (nm)
CCN-BAS	1250	0.35
CCN-DMS	11000	0.446
Angles	k_ϑ (kJ/mol)	ϑ_0 (deg)
BAS-BAS-CCN	50	180
BAS-CCN-DMS	50	180
CCN-DMS-DMS	50	100
SID-BAS-CCN	50	100
Non-bonded interactions	Martini 3 energy level	
BAS(N3a)-DMS	13	
BAS(P2)-DMS	16	
SID(N4a)-DMS	16	
SI(TC5)-DMS	15	

Table SI11. Bonded parameters of the triblock connections and GSG non-bonded interactions. The first part of the table reports the bond and angle parameters between the backbone beads of the peptide (BAS), the connection bead (CCN), and the PDMS bead (DMS). The functional forms of the potentials are the same as before, and the meaning of the parameters is explained in Table SI2. The second part of the table reports the non-bonded interactions between the beads that constitute the copolymer. In particular, it shows the Martini 3 energy levels from which one can deduce the σ and ϵ of the LJ potential.

PBLG model validation

To validate our PBLG model, we took as references the densities and the intermolecular radial distribution functions⁶ of two PBLG homo-blocks with different chain lengths. In particular, we used

a melt composed of 5-units peptide chains (called PBLG₅ in the following), and a melt composed of 20-units peptide chains (PBLG₂₀). Casey Johnson² reports a density of 1.25 – 1.28 g/cm³ at 300 K and computes the CG intermolecular radial distribution functions of the backbone, side chain, and benzene ring particles in Figure 3A-F. To calculate these quantities, we used PBLG melts containing 300 chains. We obtained box lengths of about 7.5 nm and 12 nm for PBLG₅ and PBLG₂₀, respectively. From a 200 ns simulation, we computed the density and the rdf. We computed three different intermolecular rdf: between BAS beads, SID beads, and the benzene ring beads, using the ring center of mass. Table SI12 reports the results obtained for the density. Our results overestimate a bit the density, probably due to the higher self-interactions between Martini 3 beads, as one can see in Figure SI7. For the same reason, our radial distribution functions can reproduce the correct positions of the peaks, but they result higher with respect Casey Johnson’s ones.

Structure	Density (g/cm ³)	Target density (g/cm ³)
PBLG ₅ (β-strands)	1.4	1.25-1.28 g/cm ³
PBLG ₂₀ (α-helices)	1.4	1.25-1.28 g/cm ³

Table SI12. PBLG homoblocks densities. The table shows a comparison between the density values obtained with our simulations and target ones, taken from ref² for the cases of the PBLG₅ melt, composed of 5-units PBLG chains that have a β-strands secondary structure, and the PBLG₂₀ melt, composed of 20-units PBLG chains that form α-helices.

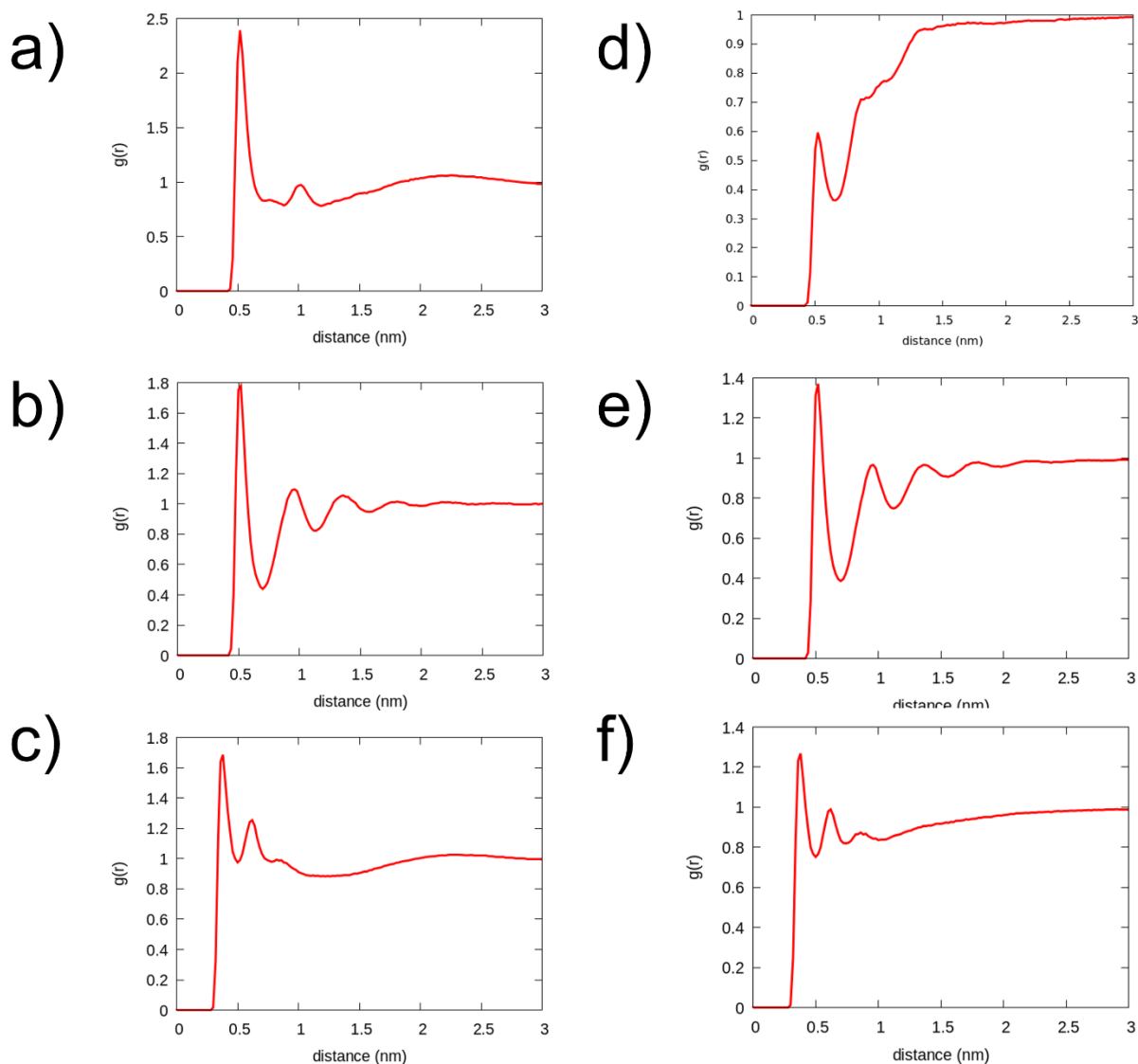


Figure S17. Intermolecular radial distribution functions (rdf) relative to the PBLG₂₀ homoblock (left column), in which the peptide chains have an α -helix secondary structure and the PBLG₅ homoblock (right column), in which the peptide chains have a β -strands structure. Panels a) and b) show the rdf relative to the backbone (BAS) beads, c) and d) the rdf of the side chain (SID) beads, e) and f) the rdf relative to the benzene rings.

Simulations set-up

We started our test with the simulation of an 8 nm GSG5 box. After a 400 ns equilibration at 300 K, we used an annealing procedure that consisted of 400 ns at 500 K and 100 ns at 300 K. The final configuration, in Figure 4c, shows a lamellar domain formation, with a domain spacing of about 7 nm. The experimental measurements report the formation of randomly oriented imperfect fibers with a diameter of 7 nm. In our simulations, whose results agree with the reference simulations, we could not achieve fiber formation because the dimensions of the box were too small.

Then, we simulated a 13 nm GSG20 box. We performed an equilibration at 300 K for 1 μ s, followed by a production run at the same temperature for 1 μ s. Then, we reduced the self-interactions between PBLG and PDMS to speed up the phase separation dynamics and performed a 1 μ s simulation annealing to 500 K. We finally reset the correct PBLG-PDMS interactions to verify that we obtained a proper configuration for the triblock. We used an annealing procedure consisting of 1 μ s at 300 K, 2 μ s at 500 K, and 600 ns at 300 K. Figure 4d shows the final configuration of the GSG20 triblock, with the formation of hexagonally packed PDMS cylinders, as expected from the experiments. As in ref⁶, we obtained a domain spacing of about 13 nm, comparable with the experimental value of 10 nm.

As one may notice, the simulation times needed to obtain the correct configurations were much longer than those of reference⁶, because of the different choices in the PBLG-PDMS non-bonded interactions. Casey Johnson used $\epsilon_{PBLG-PDMS} = 0.1$ kcal/mol to simulate the strong segregation limit between PDMS and PBLG. However, this tiny interaction strength, which allows obtaining the desired morphology in 280 ns, is incompatible with the Martini ϵ values. In our case, we used the more physical energy levels of the Martini 3 force field, which provided a slower phase separation.

Notes and references

- (1) Smith, J. S.; Borodin, O.; Smith, G. D. A Quantum Chemistry Based Force Field for Poly(Dimethylsiloxane). *J. Phys. Chem. B* **2004**, *108* (52), 20340–20350. <https://doi.org/10.1021/jp047434r>.
- (2) GROMACS development team. GROMACS Documentation Release 2020. **2020**.
- (3) Arrighi, V.; Gagliardi, S.; Dagger, A. C.; Semlyen, J. A.; Higgins, J. S.; Shenton, M. J. Conformation of Cyclics and Linear Chain Polymers in Bulk by SANS. *Macromolecules* **2004**, *37* (21), 8057–8065. <https://doi.org/10.1021/ma049565w>.
- (4) Shi, W.; Siefert, N. S.; Morreale, B. D. Molecular Simulations of CO₂, H₂, H₂O, and H₂S Gas Absorption into Hydrophobic Poly(Dimethylsiloxane) (PDMS) Solvent: Solubility and Surface Tension. *J. Phys. Chem. C* **2015**, *119* (33), 19253–19265. <https://doi.org/10.1021/acs.jpcc.5b05806>.
- (5) Ibarboure, E.; Papon, E.; Rodríguez-Hernández, J. Nanostructured Thermotropic PBLG-PDMS-PBLG Block Copolymers. *Polymer (Guildf)*. **2007**, *48* (13), 3717–3725. <https://doi.org/10.1016/j.polymer.2007.04.046>.
- (6) Johnson, J. C.; Korley, L. T. J.; Tsiges, M. Coarse-Grained Modeling of Peptidic/PDMS Triblock Morphology. *J. Phys. Chem. B* **2014**, *118* (47), 13718–13728. <https://doi.org/10.1021/jp506553v>.
- (7) Knecht, V.; Reiter, G.; Schlaad, H.; Reiter, R. Structure Formation in Langmuir Peptide Films As Revealed from Coarse-Grained Molecular Dynamics Simulations. *Langmuir* **2017**, *33* (26), 6492–6502. <https://doi.org/10.1021/acs.langmuir.7b01455>.

